Data Supplement item IV for
Ring et al. 2024

The Samail subduction zone dilemma: Geochronology of high-pressure rocks from the Saih Hatat window, Oman, reveals juxtaposition of two subduction zones with contrasting thermal histories. Earth Science-reviews

Rb-Sr isotopic dating

Methods

The Rb-Sr multimineral approach is a powerful tool to directly date HP assemblages and also the waning stages of ductile deformation. The Rb-Sr isotopic clock is set at the end of simultaneous (re)crystallization processes of high-Rb/Sr minerals (mica phases, K-feldspar) in equilibrium with coexisting low-Rb/Sr phases (calcite, plagioclase, apatite). Isochron ages directly date the crystallization of a paragenesis, or the end of dynamic recrystallization after ductile shearing, provided that no later thermal-diffusive or fluid-related retrogressive overprint occurred (Inger and Cliff, 1994; Freeman et al., 1998). Muscovitic/phengitic white mica is particularly useful because resetting of its Rb-Sr system via diffusion at static conditions only occurs at temperatures >600°C (Glodny et al., 2008a). In contrast, dynamic recrystallization may reset Rb-Sr systematics in white mica in many lithologies at temperatures as low as ~300°C (Müller et al., 2000). White mica is typically analysed in several grain-size or density fractions, to test for the potential presence of inherited mica porphyroclasts. Because the shear strength of minerals is grain-size sensitive (Platt and Behr, 2011), large mica crystals tend to form textural and isotopic relics related to earlier crystallization or deformation episodes. Late-stage deformation is then preferentially partitioned into trails of fine-grained material surrounding these relics. This results in more efficient Rb-Sr isotopic resetting of smaller grains, particularly during late stages of ductile deformation. Therefore, the apparent ages of small mica grain-size fractions correspond most closely to the latest stages of ductile deformation in a given sample and provide maximum ages for the end of ductile deformation. Absence of systematic correlations between mica grain sizes and apparent ages indicate penetrative recrystallization, facilitating straightforward dating of the latest stages of a distinct mylonitization event.

For mineral separation, we used small samples of less than 100 g, to avoid larger-scale compositional and isotopic heterogeneities. Rb-Sr isotopic data were generated at GFZ Potsdam on a Thermo Scientific TRITON TIMS instrument. Sr isotopic compositions were measured in dynamic multicollection mode, whereas Rb isotope dilution analyses were done in static

multicollection mode. The value obtained for $^{87}Sr/^{86}Sr$ in the NIST SRM 987 reference material during the period of analytical work was 0.710242 ± 0.000020 (2σ, n = 16). For calculation of isochron parameters, standard uncertainties of ±0.005% for Sr isotopic ratios and of ±1.5% for Rb/Sr ratios were used. Handling of mineral separates and analytical procedures are described in more detail in Glodny et al. (2008). Uncertainties of isotope and age data are quoted at 2σ throughout this work. The program ISOPLOT/ EX3.71 (Ludwig, 2009) was used to calculate regression lines. The ^{87}Rb decay constant is used as recommended by Villa et al. (2015).

Descriptions of samples used for Rb-Sr age dating

OM19-1 (23°34'32"N, 58°32'59"E)

Carpholite-bearing calcphyllite of Ruwi Nappe

Very fine-grained, shiny, strongly deformed calcphyllite; a typical photo of the rock is shown in Fig. 6e of the main paper.

Assemblage: white mica (near 90%), minor quartz, chlorite, carbonate, feldspar (?), rare carpholite (which was difficult to separate from oxides).

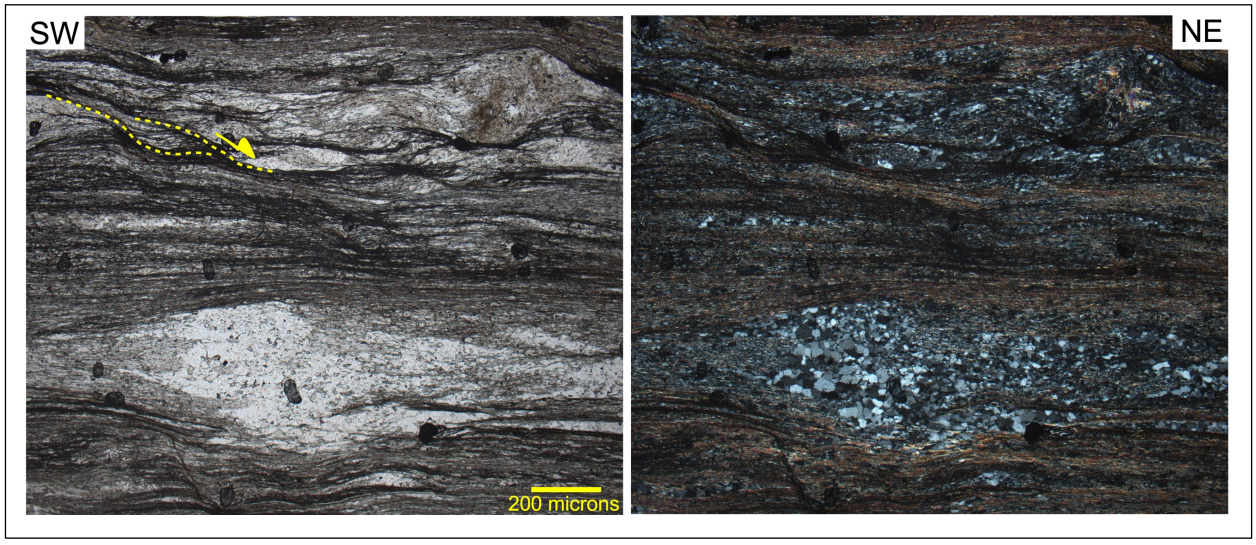

Fig. III-1. (a) Plane- (PPL) and (b) cross-polarized-light (XPL) images of OM19-1 thin section. Note fine grain size and top-NE shear bands, especially in upper left of photographs.

OM19-5 (23°28'08"N, 58°42'22"E)

Initial decompression of eclogite from As Sifah Nappe (As Sifah Unit)

Medium-grained, strongly sheared high-P rock; mm-thick layers have an enrichment of glaucophane + chlorite; see Fig. 6f of main paper.

Assemblage: glaucophane, garnet (partly retrogressed), white mica, omphacite (partly retrogressed), rutile, apatite, carbonate (colorless and yellowish), quartz (?).

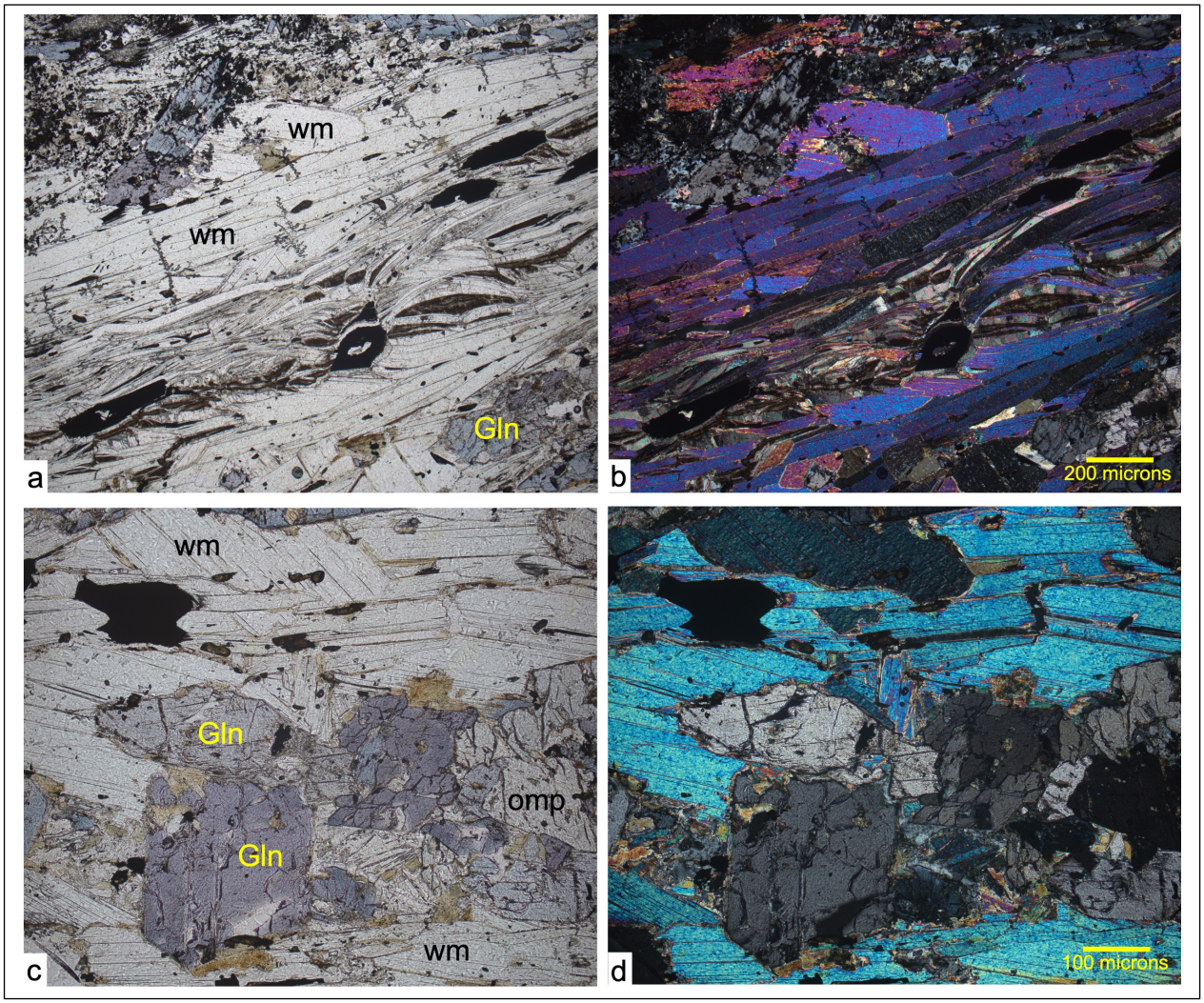

Fig. III-2. (a, c) PPL and (b, d) XPL thin-section microphotographs of sample OM19-5. (a, b) Bands of relatively coarse-grained white mica and glaucophane alternating with sheared white mica layers enriched with opaques. (c, d) Coarse-grained layer of white mica, glaucophane and omphacite with some late growth of oxychlorite (brownish-green mineral).

OM19-6 (23°27'33"N, 58°46'49"E)

Greenschist-facies retrogression of eclogite from As Sifah Nappe (As Sifah Unit)

Fairly coarse-grained, distinctly reddish, foliated rock with abundant top-NE shear bands; rich in white mica, quartz, chlorite. See Fig. 6g in main paper.

Assemblage: white mica, quartz, opaques (hematite), apatite (rare), chlorite, feldspar (? rare), no garnet, glaucophane or omphacite.

OM19-8 (23°27'36"N, 58°45'39"E).

Felsic, high-P quartz-mica schist from As Sifah Nappe (As Sifah Unit)

Felsic, quartz-rich, strongly foliated schist, with cm-sized elongated aggregates of white mica; rich in iron-poor calcite.

Assemblage: white mica, quartz, glaucophane (present but rare) epidote (present but rare), rutile, calcite, minor ankerite, apatite.

OM19-9 (23°23'35"N 58°45'09"E).

Greenschist-facies mylonite from Hulw Nappe (As Sheik Unit)

Strongly foliated, fine-grained rock, silvery-phyllitic appearance, chloritoid porphyroblasts; see Fig. 6k of main paper.

Assemblage: white mica, quartz, chloritoid, blackish phase (LBRF (floating in $CHBr_3$, i.e., density <2.83, and slightly paramagnetic), apatite, minor biotite group mineral (golden colored, shiny).

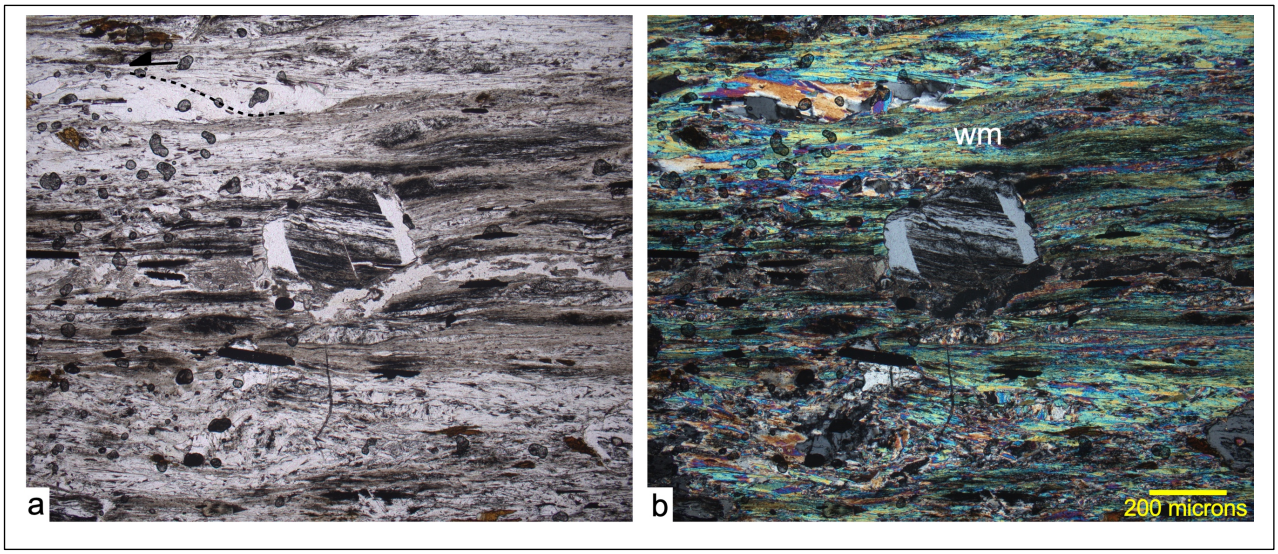

Fig. III-3. (a, b) PPL and XPL thin-section microphotographs of sample OM19-9. Fine-grained, white-mica-rich groundmass with slightly asymmetric chloritoid porphyroblast.

OM19-13 (23°28'52"N, 58°45'10"E)

Top-NE As Sheik shear zone at Hulw/As Sifah nappe boundary

Fine- to medium grained, white-mica rich mylonitic calcschist; Fig. 6j in main paper.

Assemblage: carbonate (white), carbonate (yellow), white mica, quartz (?), apatite, minor rutile.

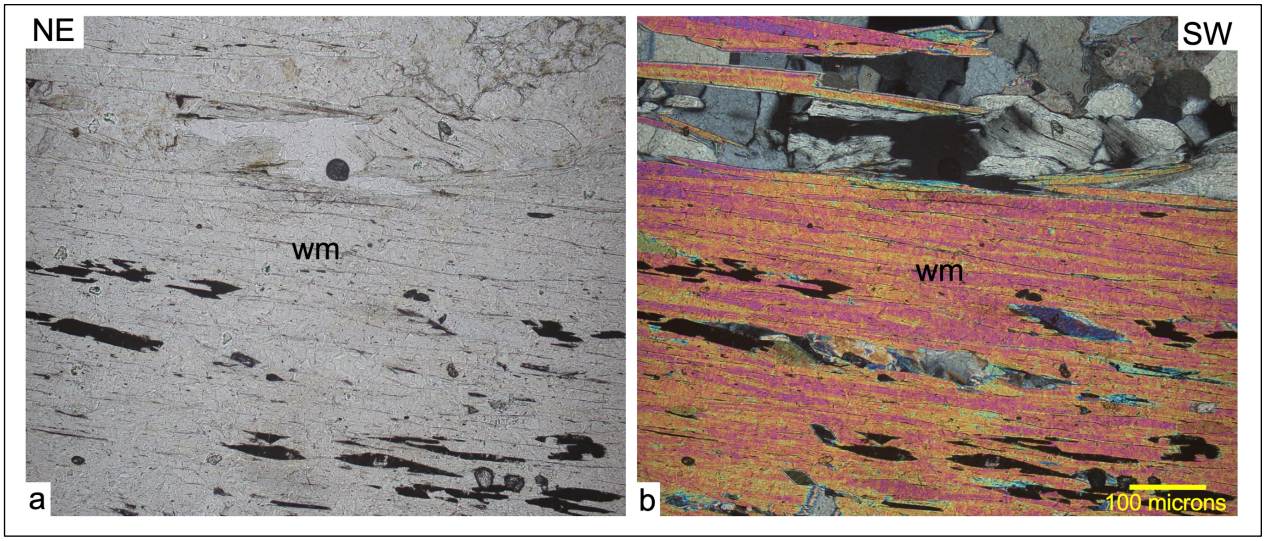

Fig. III-4. (a, b) PPL and XPL thin-section microphotographs of sample OM19-13. Bands basically composed of white mica alternate with quartz-calcite layers.

OM19-14 (23°29'19"N, 58°44'30"E)

Top-NE shear zone at Upper/Lower-Plate Discontinuity (boundary between Hulw (As Sheik Unit) and Khuryan-Quryat-Mayh-Saih Hatat (KQMS) Nappe)

Fine to medium-grained, white-mica rich mylonitic calcschist; sample seems to be pervasively oxidized (hematite); see Fig. 6l in main paper.

Assemblage: calcite (Fe-poor), white mica, quartz, hematite (in aggregates), glaucophane.

OM19-17 (23°27'31"N, 58°40'22"E)

Blueschist from Hulw Nappe (Hulw Unit)

Fine- to medium-grained, strongly foliated blueschist; potentially post-kinematic growth of glaucophane; sample shows cm-scale layering: glaucophane-rich layers alternate with quartz-albite-epidote layers.

Assemblage: glaucophane, white mica, epidote, quartz, feldspar (albite?), apatite, minor titanite, chlorite.

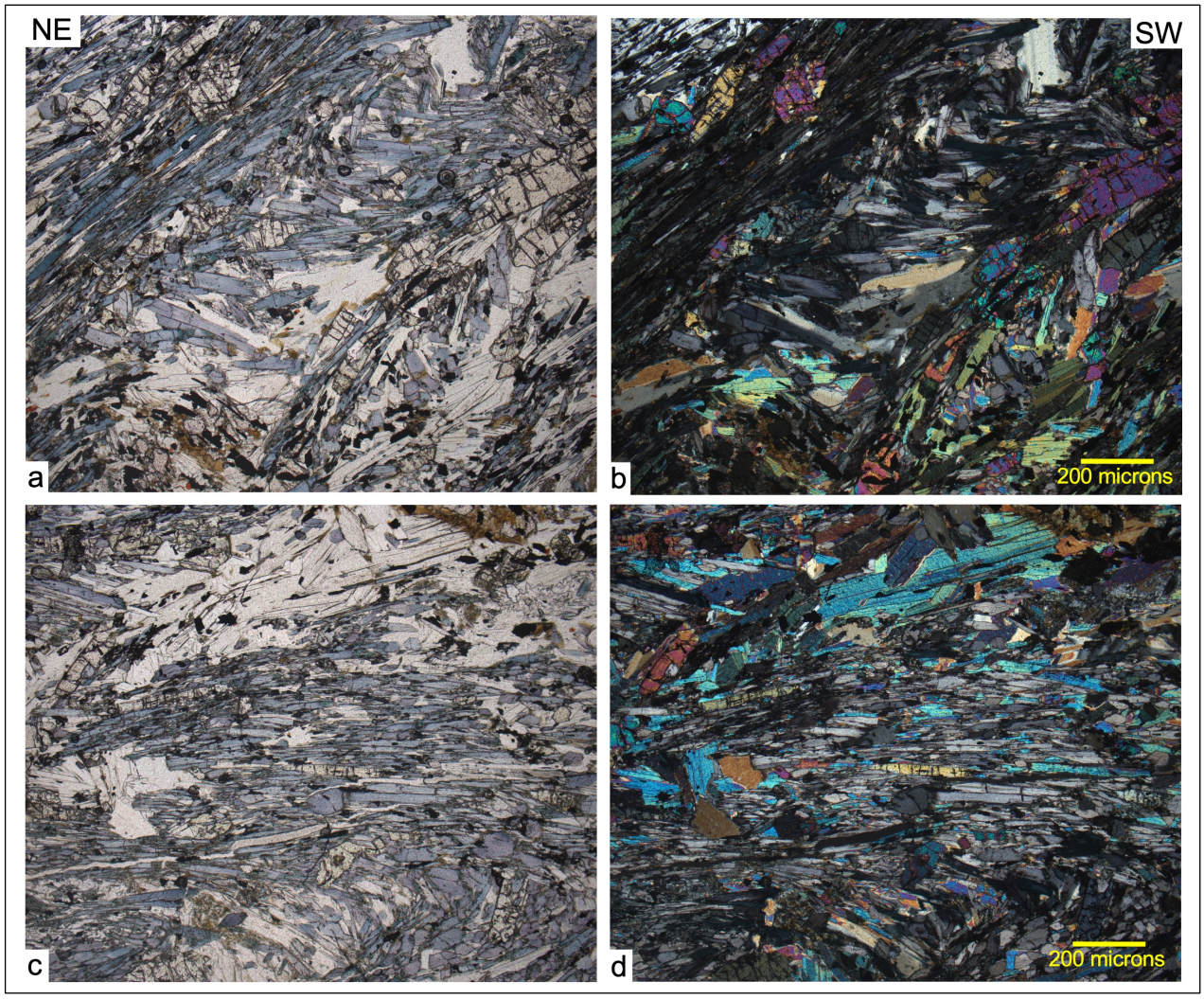

Fig. III-5: (a, c) PPL and (b, d) XPL thin-section microphotographs of sample OM19-17. Glaucophane-rich rock with epidote and white mica.

OM19-18 (23°27'56"N, 58°45'25"E)

Blueschist As Sifah Nappe (Diqdah Unit)

Dark, medium-grained schist, with felsic layers and nests/ghosts of garnet.

Assemblage: quartz, glaucophane, omphacite, garnet, epidote, white mica, titanite, apatite, chlorite.

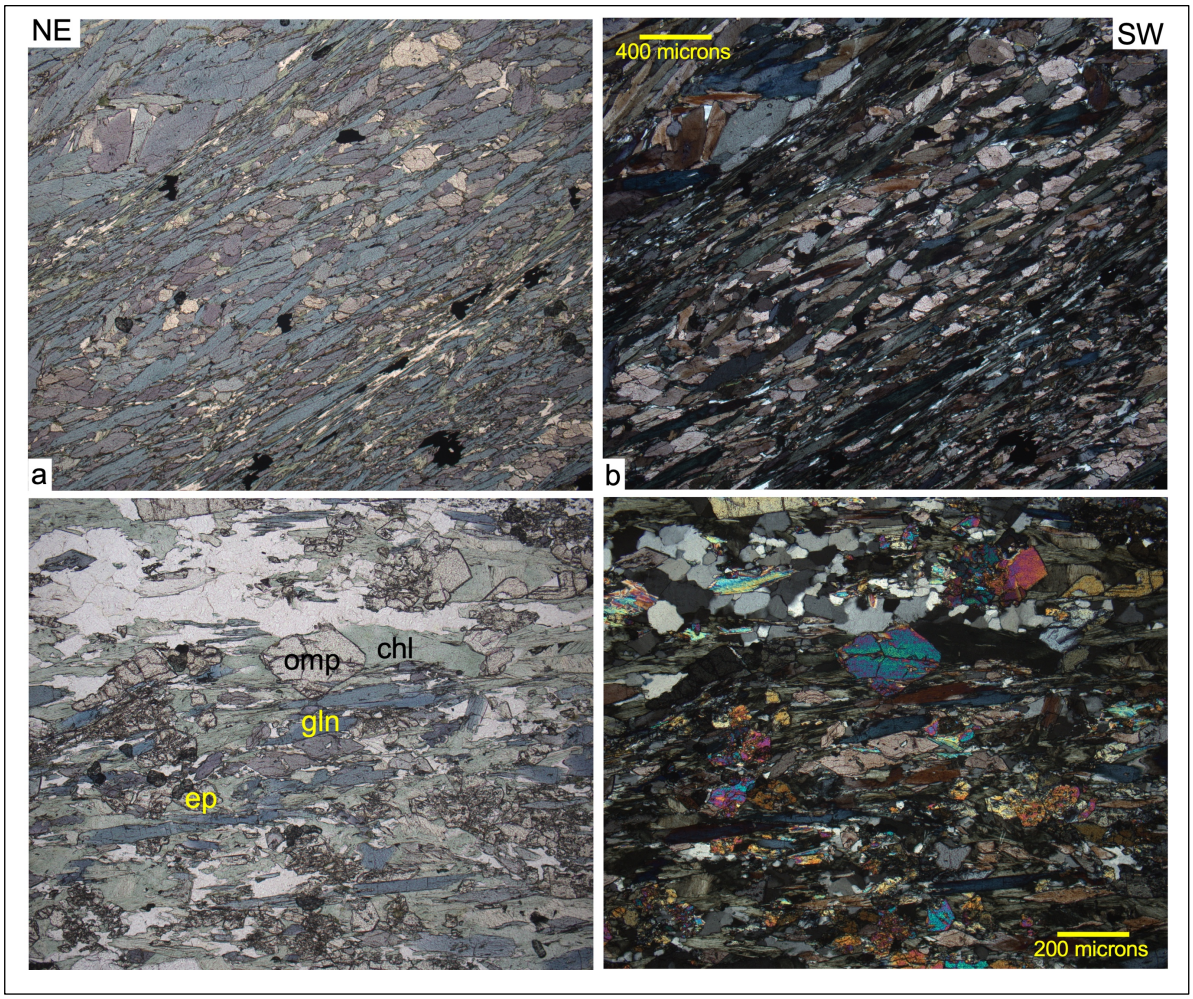

Fig.III-6. (a, c) PPL and (b, d) XPL thin-section microphotographs of sample OM19-18. (a, b) Bands of medium-grained glaucophane alternate with more fine-grained glaucophane layers. (c, d) Omphacite with chlorite-filled strain shadows and garnet-epidote clusters.

OM19-19 (23°31'03"N, 58°42'19"E)

Yenkit shear zone

Fine-grained, yellowish, carbonate mylonite / calcschist.

Assemblage: calcite, carbonate (Fe), white mica, minor chlorite, quartz, hematite.

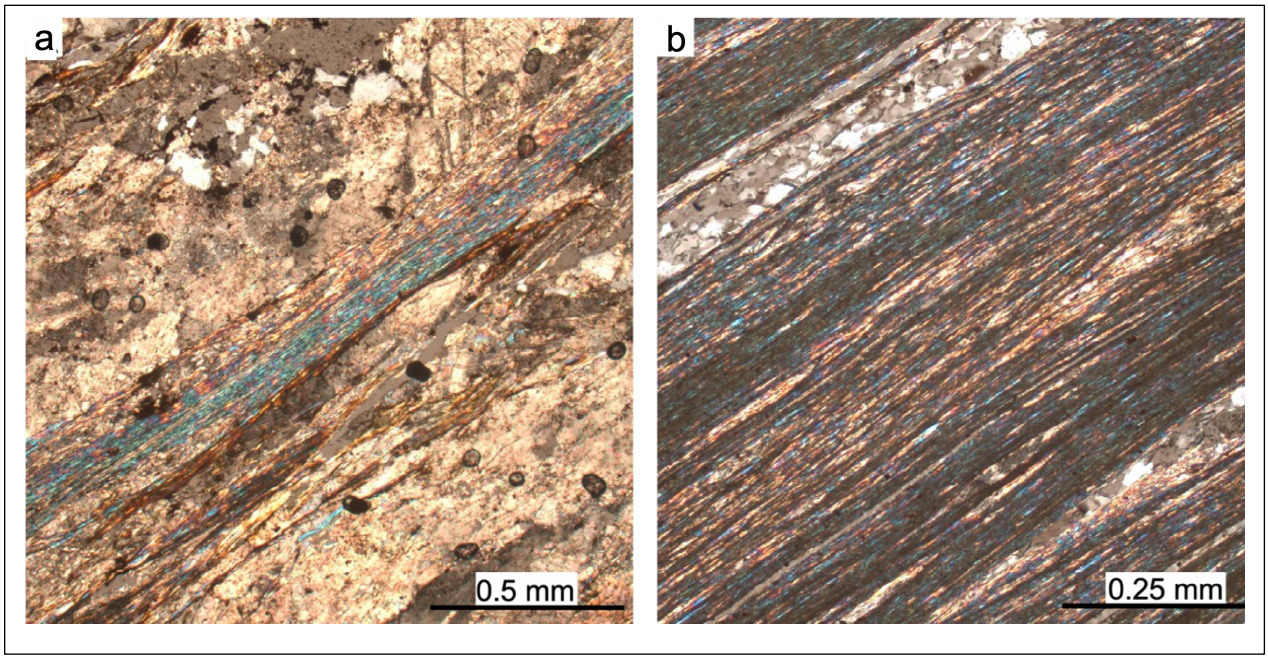

Fig.III-7. XPL photographs of sample OM19-19. (a) Calcschist that is dominating the outcrop and being made up primarily of Fe-rich carbonate with thin layers of fine-grained, thoroughly recrystallized white mica and oxychlorite. (b) Calcphyllite from very thin layers within the calcschist; the layers are primarily made up by white mica with minor chlorite; layer at top composed of carbonate and quartz.

OM22-1 (23°31'12"N, 58°42'47"E)

Yenkit shear zone

Fine-grained, yellowish, carbonate mylonite. Strong foliation is mainly defined by planar aggregates of white mica. Crystals of carbonate reach up to 0.5 mm, whereas white mica crystals are generally much smaller.

Assemblage: calcite, carbonate (Fe), white mica, minor chlorite, quartz, hematite.

Fig. III-8. Outcrop in which sample OM22-1 has been collected. About 100m thick zone of mylonite calcschist grade into less deformed rock at top of hillslope.

OM22-4 (23°30'19"N, 58°37'30"E)

Al Khuryan-Quryat-Mayh-Saih Hatat (KQMS) Nappe

Extremely fine-grained, strongly deformed carbonate schist, tightly foliated, rich in white mica, with silvery-shiny, phyllitic appearance.

Assemblage: calcite (Fe-rich and Fe-poor), white mica, minor glaucophane, chlorite, quartz, hematite.

OM22-5 (23°34'25"N, 58°32'57"E)

Yenkit shear zone

Fine-grained, strongly deformed carbonate mylonite from uppermost Al Khuryan-Quryat-Mayh-Saih Hatat (KQMS) Nappe. Foliation is defined on a mm scale by alternation of almost pure carbonate layers with thin (<1 mm) more sheet-silicate rich layers.

Assemblage: calcite, dolomite, white mica.

Fig. III-9. Sample OM22-5, tightly foliated carbonate mylonite marking contact between Al Khuryan-Quryat-Mayh-Saih Hatat (KQMS) and Ruwi nappes E Al Hamriyah.

OM22-7 (23°30'27"N, 58°40'24"E)

Yenkit shear zone

Reddish calcite mylonite from Al Khuryan-Quryat-Mayh-Saih Hatat (KQMS) Nappe

Fine-to medium grained, strongly deformed rock with slightly undulated foliation planes.

Assemblage: calcite, dolomite, white mica, quartz, hematite.

OM22-8 (23°30'47"N, 58°41'53"E)

Al Khuryan shear zone

Fine-grained, dark, calcite mylonite from Al Khuryan-Quryat-Mayh-Saih Hatat (KQMS) Nappe; see Fig. 6i of main paper. Extremely tight foliation with near-perfectly planar foliation planes. Assemblage: calcite, dolomite, white mica, quartz, opaques.

OM22-9 (23°35'29"N, 58°32'22"E)

Ruwi Hill shear zone

Reddish, fine grained carbonate mylonite from Al Khuryan-Quryat-Mayh-Saih Hatat (KQMS) Nappe; see Fig. 6c of main paper. Foliation is defined by interlayering of carbonate-dominated with sheet-silicate-dominated layers on a mm scale, and by near- perfect layer-parallel orientation of white mica-rich aggregates. Assemblage: calcite, dolomite, white mica, minor quartz, hematite

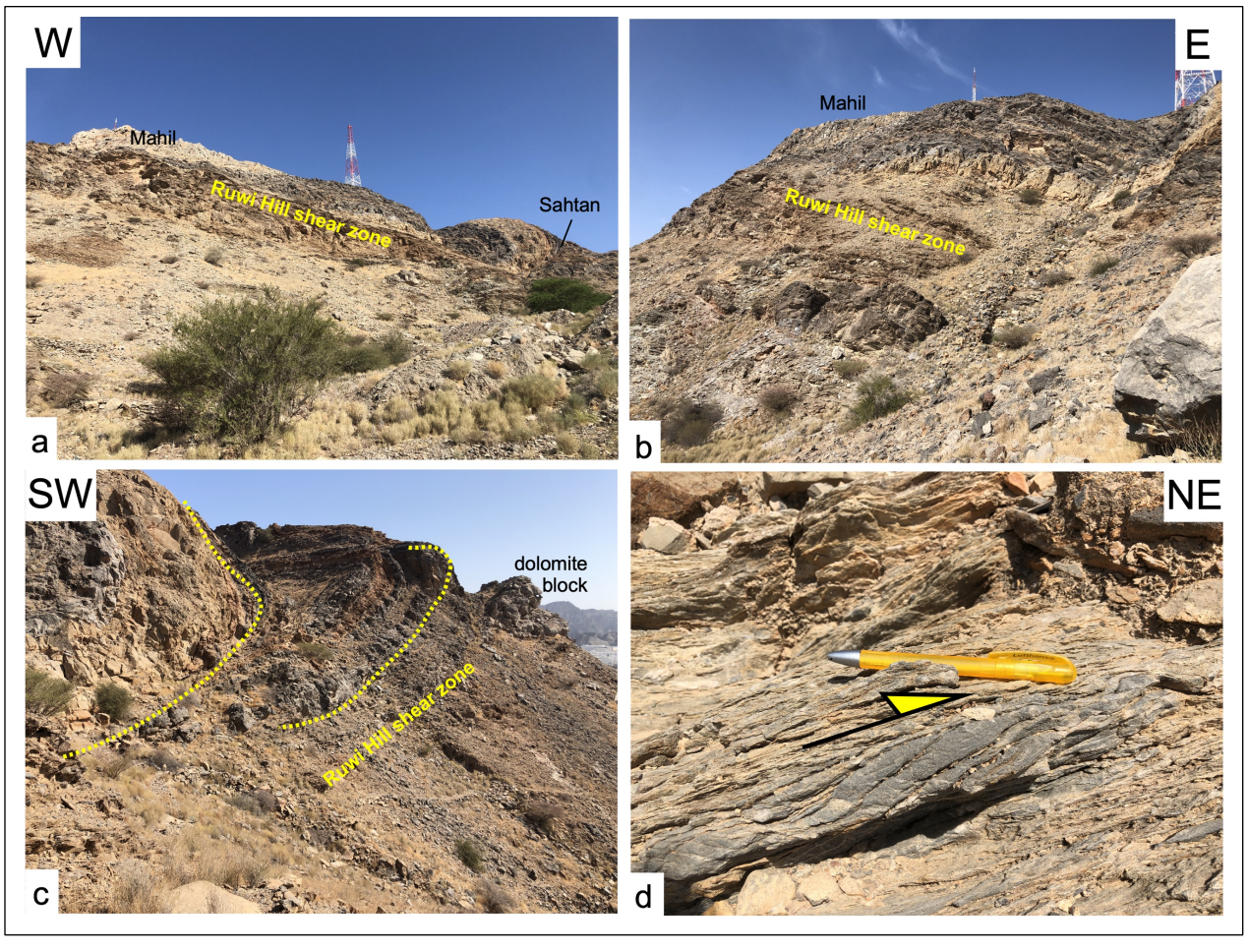

Fig. III-10. Ruwi Hill shear zone. (a, b) Panoramic E-W section showing shear zone with recumbent NE-closing fold cored by Mahil Formation. (c) Similar view of NE-closing fold. (d) Top-NE asymmetric dolomite clast in shear zone.

OM22-10 (23°34'33”N, 58°33'01”E)
Hamriyah shear zone
Reddish, fine-grained calcphyllite mylonite from uppermost Ruwi Nappe; see Fig. 6a of main paper and Fig. 23 of Hansman et al. (2021). Rock is exceptionally rich in hematite. Incipient development of foliation-parallel segregation into more sheet-silicate rich versus pure carbonate layers. Assemblage: calcite, hematite, white mica, minor quartz

OM22-16 (23°22’57”N, 58°29’37”E)
Reddish, fine-grained mica schist from Hatat schist of Saih Hatat Unit of Al Khuryan-Quryat-Mayh-Saih Hatat (KQMS) Nappe.
Assemblage: calcite, white mica, quartz, hematite.

OM23-1 (23°33’38”N, 58°31’32”E)
Extremely fine-grained, mafic, high-P schist of Saiq Formation of Hatat schist of Saih Hatat Unit of Al Khuryan-Quryat-Mayh-Saih Hatat (KQMS) Nappe. Average grain size of white mica is <10 μm; locally white mica occurs in separable, near- monomineralic aggregates of up to 200 μm in diameter.
Assemblage: calcite (Fe), white mica, glaucophane, chlorite, quartz (?), albite (?), opaques.

OM23-2 (23°30’35”N, 58°36’56”E)
Al Wudya shear zone
Reddish, fine-grained, tightly foliated carbonate-rich mylonite of Mayh Unit of Al Khuryan-Quryat-Mayh-Saih Hatat (KQMS) Nappe. Near perfectly planar foliation planes show a silvery, phyllitic appearance and are dotted with reddish carbonate aggregates.
Assemblage: calcite,Fe-rich carbonate, white mica, chlorite, opaques.

OM23-3 (23°28’47”N, 58°39’42”E)
Upper/Lower-Plate Discontinuity
Fine-grained, mafic, mylonitic schist with dark-silvery appearance and Fe carbonate and epidote porphyroblasts.
Assemblage: calcite, Fe-rich carbonate, quartz, white mica, chlorite, epidote, tourmaline, apatite, opaques.

OM23-4 (23°34’32’’N, 58°32’59’’E)

Calcphyllite of Ruwi Nappe

Fine-grained calcphyllite; see Fig. 6e of the main paper; sample collected from calcite precipitate in large top-NE shear-band structure.

Assemblage: white mica (near 90%), minor quartz, chlorite, carbonate, oxides.

Summary figure of Rb-Sr age data

Figure III-11 accompanies Figure 9 in section 4.5.2. (History of shear-zone activity) of the main article. It provides a more comprehensive illustration summarizing numerous details of the tectonic processes and their timing is provided.

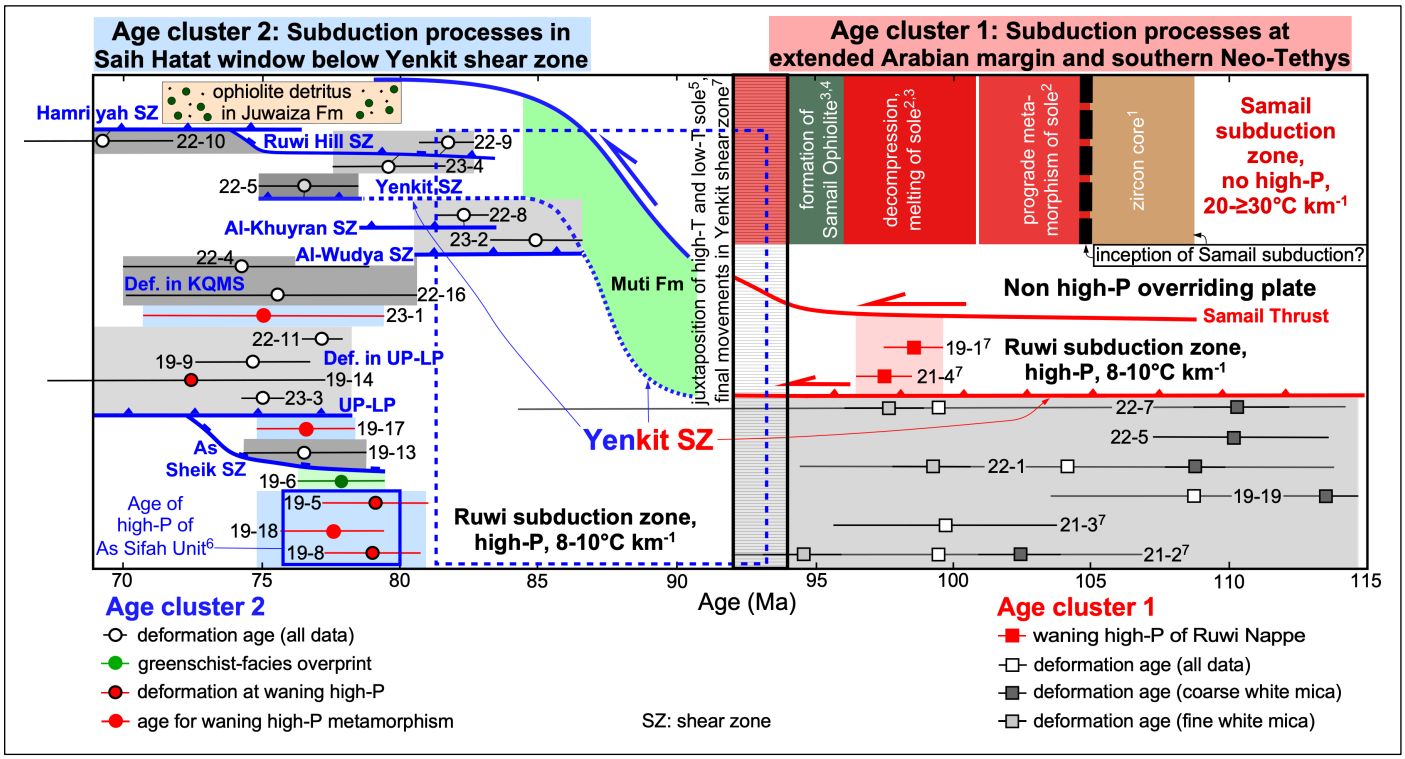

Fig.III-11. Synoptic summary showing age clusters 1 and 2 separated by deposition of syntectonic sediments of Muti Formation as part of Aruma Group; note that younger Juwaiza Formation containing ophiolite detritus also part of Aruma Group. Age cluster 1 (highlighted in red colours) highlights two-fold evolution of 'hot' (thermal gradients 20->30°C km^{-1}) Samail subduction zone and 'cold' (thermal gradients 8-10°C km^{-1}) Ruwi subduction zone; final juxtaposition of contrasting settings after 93 Ma; potential beginning of underthrusting of platform margin (possibly associated with erosion of forebulge and sedimentation of Muti Formation) indicated by dashed blue box. Age cluster 2 emphasizes subduction of high-P nappes of Saih Hatat window in Ruwi subduction zone. Explanation: [1]Garber et al. (2020), [2]Guilmette et al. (2018), [3]Rioux et al. (2021), [4]Tilton et al. (1981), [5]Hacker et al. (1997), [6]El-Shazely et al. (1997), Warren et al. (2003, 2005), Garber et al. (2021), [7]Ring et al. (2023). Gray background colours indicate deformation, blue box at bottom left high-P metamorphism at 80-76 Ma, dashed blue box shows deformation in Al Khuryan and Al Wudya shear zone representing oldest mylonitization ages of age cluster 2. See main text for interpretation.

References:

Freeman, S.R., Butler, R.W.H., Cliff, R.A., Rex, D.C. (1998). Direct dating of mylonite evolution: a multi-disciplinary geochronological study from the Moine Thrust Zone, NW Scotland. J. Geol. Soc. London, v. 155, p. 745–758. https://doi.org/10.1144/ gsjgs.155.5.0745.

Glodny, J., Ring, U., Kühn, A. (2008). Coeval high-pressure metamorphism, thrusting, strike-slip, and extensional shearing in the Tauern Window, Eastern Alps. Tectonics, 27. https://doi.org/10.1029/2007TC002193.

Hansman, R.J. et al. (2021). Structural architecture and Late Cretaceous exhumation history of the Saih Hatat Dome (Oman), a review based on existing data and semi-restorable cross-sections. Earth-Science Reviews, 217, https://doi.org/10.1016/j.earscirev.2021.103595.

Inger, S., Cliff, R.A. (1994). Timing of metamorphism in the Tauern Window, Eastern Alps: Rb-Sr ages and fabric formation. J. Metamorph. Geol., v. 12, p. 695–707.

Ludwig, K.R. (2009). Isoplot/Ex Ver 3.71: A Geochronological Toolkit for Microsoft Excel. Berkeley Geochronology Center Special Publication, Berkeley.

Müller, W., Mancktelow, N.S., Meier, M. (2000). Rb-Sr microchrons of synkinematic mica in mylonites: An example from the DAV fault of the Eastern Alps. Earth Planet. Sci. Lett. 180, 385–397.

Platt, J.P., Behr, W.M. (2011). Grainsize evolution in ductile shear zones: Implications for strain localization and the strength of the lithosphere. J. Struct. Geol. 33, 537–550.

Villa, I.M., De Bièvre, P., Holden, N.E., Renne, P.R. (2015). IUPAC-IUGS recommendation on the half life of 87Rb: Geochimica et Cosmochimica Acta, 164, 382– 385, doi: 10.1016/j.gca.2015.05.025.